Air-filled square coaxial transmission line and its use in microwave filters

I. Llamas-Garro, M.J. Lancaster and P.S. Hall

Abstract: A suspended coaxial transmission line with an air propagation medium is presented. The transmission line is made only of metal, thereby avoiding dielectric and radiation losses. Short-circuit stubs suspend the centre conductor of the coaxial structure which is used in the design of two dual-mode narrowband microwave filters. Stacked layers of copper sheets are used to form the square coaxial transmission line, which has low loss and low dispersion.

1 Introduction

There is currently considerable interest in using micromachining technology in the implementation of microwave and millimetre-wave passive circuits and numerous structures have been presented in the literature. The objective is to have a micromachined structure which has low propagation loss and can be fabricated using currently available processes. The structures should also be able to be easily integrated with other passive and active components.

Coaxial transmission lines are compact in size, and present low loss and low dispersion, making them a suitable structure for the design of millimetre-wave circuits. At millimetre-wave frequencies the use of low loss and low dispersion micromachined devices has mainly been targeted on the investigation of suspended microstrip lines [1–3]. The thin centre conductor of the microstrip is usually suspended by thin membranes. The layered coaxial structure proposed here is more compact and has outstanding low loss characteristics [4], compared with [1–3]. One of the few structures that exhibits lower loss is the rectangular waveguide. However, at the frequencies of interest, this is too large for micromachining processes and is also unsuitable for many applications because of its size. The air-filled coaxial cable has the advantages of small size and low dispersion compared with the waveguide, and has an air propagation medium and high power characteristics. An air-filled square coaxial transmission line can be optimised to give a low attenuation constant by using a highly conducting metal and by choosing an appropriate cross-section for the coaxial line.

The complete filter is shown in Fig. 1*a*. It is fabricated from five conducting plates. Layer 3 is the middle layer and contains the centre conductor of the square coaxial cable. A plan view of this layer is shown separately in Fig. 1*b*, and consists of an input feed line which is supported by quarter-wavelength stubs which are grounded. There is then a capacitive gap between the feed line and the resonator. After the resonator there is another capacitive gap to the output transmission line. The design of the dual-mode filter is presented in Section 3 and details of the stub-suspended transmission line can be found in [5]. The other layers in Fig. 1*a* form the outer conductor, with layers 2 and 4 providing the sidewalls and layers 1 and 5 forming the top and bottom of the coaxial cable.

In order to demonstrate these ideas, two suspended dual-mode narrowband filters having a 1% fractional bandwidth

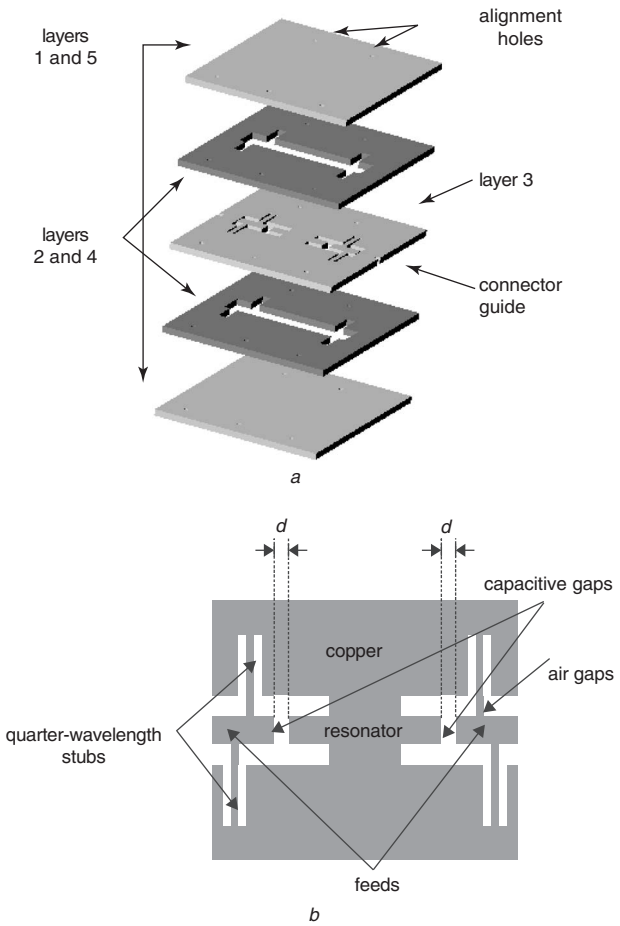

Fig. 1 *Layered coaxial filter*
a Five-layer coaxial assembly
b Top view of layer 3, showing the centre conductor of the coaxial cable filter

IEE Proceedings online no. 20041159
doi:10.1049/ip-map:20041159
Paper first received 22nd March and in revised form 6th August 2004

The authors are with the Department of Electronic, Electrical and Computer Engineering, School of Engineering, The University of Birmingham, Birmingham, B15 2TT, UK
E-mail: llamasi@iee.org

(FBW) centred at 9.1 and 29.75 GHz will be presented; the Ka-band filter has potential application in a local area multipoint distribution system.

2 Design of square-cross-section cables

To obtain a low-loss coaxial transmission line, for a given operating frequency range, the cross-sectional area of the coaxial structure should be optimised. Figure. 2 shows an air-filled square coaxial transmission line. The appropriate choice of cross-section to be used in a specific design is a trade-off between having a low attenuation constant for the transmission line and predicting at what frequency the higher modes will start to propagate. When higher modes are present, these lead to a dispersive transmission line, so for most applications it is desired to propagate only a TEM mode. Information to calculate the presence of non-TEM modes in square coaxial lines are given in [6].

The impedance of the square coaxial line in Fig. 2, can be calculated by [7]:

$$Z_O = \frac{47.09}{\sqrt{\varepsilon_r}} \frac{(b-w)}{(0.2794b + 0.7206w)} \quad \text{for } b/w < 2.5 \qquad (1)$$

$$Z_O = \frac{136.7}{\sqrt{\varepsilon_r}} \log_{10}\left(0.9259\frac{b}{w}\right) \quad \text{for } 2.5 \le b/w \le 4 \qquad (2)$$

$$Z_O = \frac{138.06}{\sqrt{\varepsilon_r}} \log_{10}\left(0.914\frac{b}{w}\right) \quad \text{for } b/w > 4 \qquad (3)$$

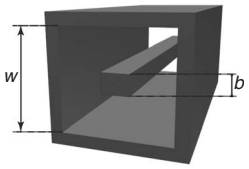

Fig. 2 *Air-filled square coaxial transmission line*

The attenuation constant due to conductor loss for the square coaxial line, can be calculated by [7]:

$$\alpha_c = \frac{47.09R_s}{\eta_o Z_O}\left(1+\frac{b}{w}\right) \times \frac{w}{(0.2794b + 0.7206w)^2} \quad \text{for } b/w < 2.5 \qquad (4)$$

$$\alpha_c = \frac{59.37R_s}{\eta_o Z_O}\left(1+\frac{b}{w}\right)\frac{1}{b} \quad \text{for } 2.5 \le b/w \le 4 \qquad (5)$$

$$\alpha_c = \frac{59.96R_s}{\eta_o Z_O}\left(1+\frac{b}{w}\right)\frac{1}{b} \quad \text{for } b/w > 4 \qquad (6)$$

To choose the appropriate size for the cross-section of a transmission line, the following factors need to be taken into account. A larger cross-sectional area for the line has the benefit of having a low attenuation constant, as shown in Fig. 3*e*. For the coaxial filters discussed in this paper, it is desired to propagate only a TEM mode, which is the lowest-order mode in a coaxial line. We will design out transmission line in such a way that the frequencies at which the higher-order modes begin to propagate is above the filter operating frequency, which now limits the size of the cross-section.

Before moving on to the detailed discussion of the design it is interesting to compare the conductor losses of various types of transmission line to justify our choice of a square coaxial cable. This comparison is shown in Fig. 3. Different transmission line cross-sections are considered in Fig. 3, these are the round coaxial (Fig. 3*a*), the square coaxial, (Fig. 3*b*), the microstrip (Fig. 3*c*) and the stripline (Fig. 3*d*). All transmission lines illustrated in Fig. 3 are air-filled and we assume that there are no radiation losses, since it is common practice to have a completely shielded microstrip or stripline. The cross-sectional area considered for the microstrip and stripline were chosen to be approximately those that can be used in a practical transmission line. In smaller areas coupling between adjacent microstrips can become very important. This is a little arbitrary but gives an

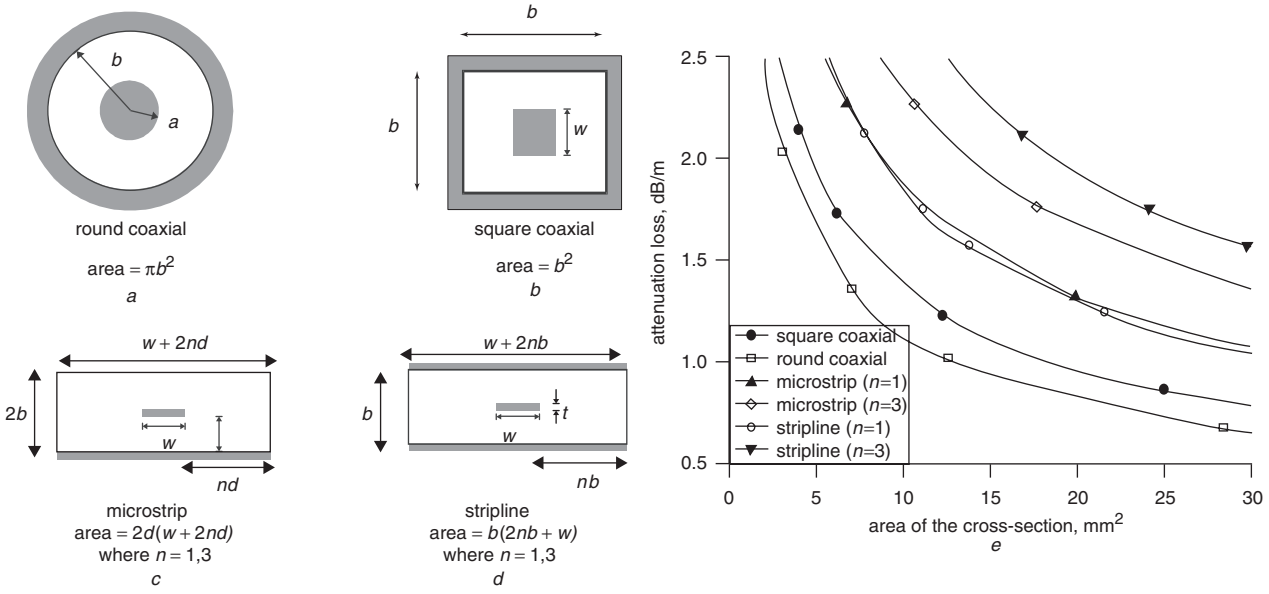

Fig. 3 *Various different types of transmission line*
a Cross-section of a round coaxial cable
b Cross-section of a square coaxial cable
c Cross-section for a microstrip line
d Cross-section for a stripline transmission line
e Attenuation loss as a function of area for each transmission line

estimate for the comparison. The thickness of the centre conductor assumed for the microstrip and stripline is taken to be 10 μm, which is many skin depths at the comparison frequency of 29.5 GHz. The computed attenuation loss due to the conductor, for 50 Ω transmission lines, with different cross-sectional areas is represented by the lines in Fig. 3*e*. Here we can see that the lowest attenuation is for the round coaxial cable, this is because it has a smooth surface-current distribution compared with the square coaxial cable, but the square cable is easier to fabricate using planar machined layers as discussed in this study. The formulas to calculate the attenuation constant for the round coaxial cable can be found in [8], and the formulas to calculate the attenuation constant for the microstrip and the stripline can be found in [9].

For the Ka-band filter described in this paper, the 50 Ω feed lines have a total area of 5.88 mm^2. This gives an attenuation of approximately 1.5 dB/m; the non-TEM modes begin to propagate at approximately 44 GHz. Similarly, for the X-band filter, the 50 Ω feed lines have a total area of 81 mm^2; this gives an attenuation of approximately 0.053 dB/m, and for this size the non-TEM modes begin to propagate at approximately 14 GHz. The simulations to obtain the theoretical response of the filters discussed in this paper were all performed using HFSS [10], and all simulated responses assumed perfect conductors to reduce the computation time.

3 Dual-mode filter design

The design procedure of the dual-mode filter follows a conventional filter design method, which starts with a low-pass prototype filter. The initial g values are then calculated from these, a band-pass transformation can be applied and the coupling coefficients between the modes of the resonator (k_c), and the external quality factor (Q_e) can be calculated. This general design procedure can be used regardless of the physical shape of the filter, and is described in [11]. The dual-mode filters were designed to have a narrow bandwidth and the following design issues were taken into account. An increase in the number of resonators makes the insertion loss increase for a given bandwidth, and it should also be mentioned that as the bandwidth gets narrower, for a given filter topology, the filter insertion loss increases. The dual-mode design presented is a compact, low loss way to achieve this bandwidth inside an air-filled coaxial cable. The g values of the low-pass filter were chosen to have a small pass-band ripple at the sacrifice of filter roll-off outside the pass-band. The filters were designed to have a 0.01 dB band-pass ripple, and a 1% FBW at 9.1 and 29.75 GHz. Both have a Chebycheff response. The low-pass prototype g values, the coupling between the two resonant modes of the resonator, and the external quality factor are summarised in Table 1.

The cross-shaped resonator is shown in Fig. 4; it supports itself in the coaxial transmission line by using the two stubs that fix it in the middle of the cable and keep it grounded to

Table 1: Design parameters for the dual-mode filters

Filter low-pass element g values		
$g_1 = 0.4488$	$g_2 = 0.4077$	$g_3 = 1.1007$
Q_e and the coupling between modes		
$Q_{eA} \approx$	$Q_{eB} = 44.88$	$k_c = 0.023$

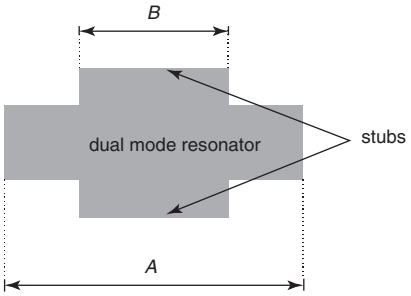

Fig. 4 *Plan of layer 3 of the filter in Fig. 1, showing just the dual-mode resonator*

the walls, as shown in Fig. 1. The coupling between the two resonant modes of the resonator is controlled by modifying the dimensions A and B in Fig. 4.

The coupling coefficient between the resonant modes can be calculated using a full-wave simulation of the whole structure [10], by varying the dimensions A and B of the resonator. If the dual-mode resonator is simulated with particular values of A and B, the output from the simulation for S_{12} would be similar to that in Fig. 5. The two peaks are caused by the interaction of the two resonant modes. From Fig. 5, the coupling coefficient is given by [11]:

$$k_{ij} = \frac{f_2^2 - f_1^2}{f_2^2 + f_1^2} \tag{7}$$

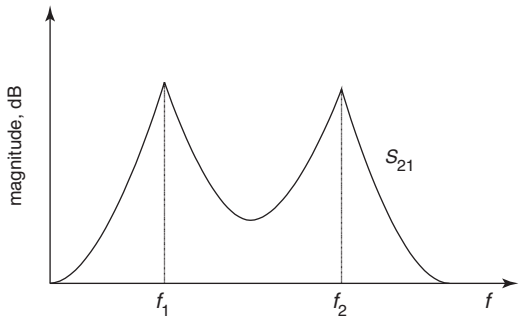

Fig. 5 *S_{21} simulated response for the dual-mode resonator*

where f_1 and f_2 are the frequencies of the two coupled peaks. By performing several separate simulations with different values of A and B it is possible to produce the graphs shown in Fig. 6. These are for the Ka-band filter, for different resonator dimensions, similar graphs can be obtained for the X-band filter. Once this data has been produced it is easy to read off a value of A and B to match with the coupling coefficient k_c in Table 1. The size of the capacitive gap (dimension d in Fig. 1*b*), between the resonator and the feed line needs to be adjusted to obtain the required external Q, this is done in a similar way to the coupling coefficients and is detailed in [11]. The dimensions of layer 3 for the filters discussed in this paper are shown in Fig. 7. It should be noted that there is a slight difference in the input and output of both filters; this is because the Ka-band filter is designed in such a way that a K connector can be mounted directly onto the structure.

A self-supported feed line was designed to provide input and output connections to the dual-mode filter. The design consists of a 50 Ω transmission line supported by two quarter wavelength stubs, as shown in Fig. 8*a*. The stubs are

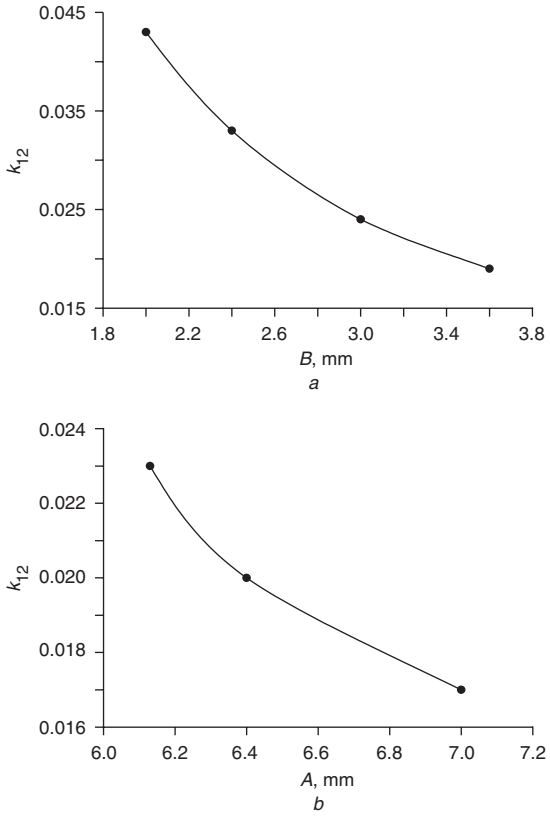

Fig. 6 *Coupling coefficient for the Ka-band filter*
a When *A* is fixed to 6 mm
b When *B* is fixed to 3 mm

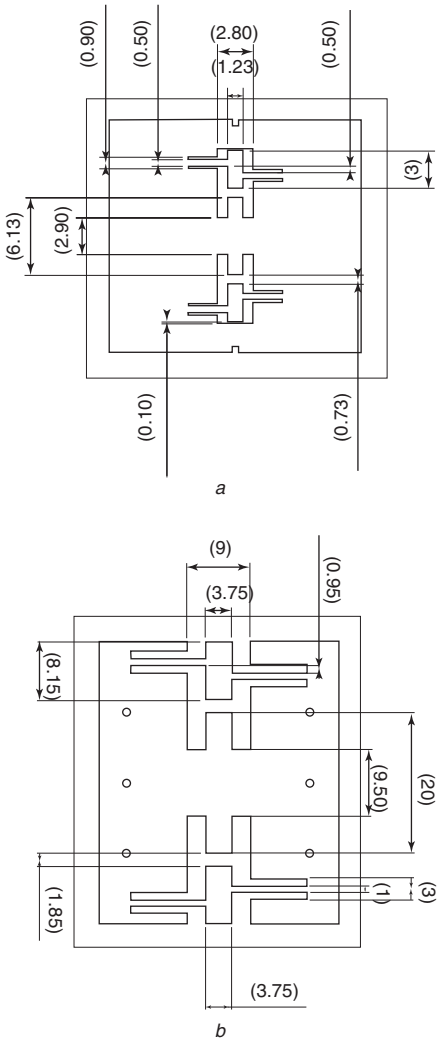

Fig. 7 *Dimensions of layer 3*
All dimensions are in mm
a Ka-band filter
b X-band filter

one-quarter wavelength long at the centre frequency of the filters, since this will achieve a good open circuit at the point where it supports the transmission line at the centre frequency of the filter. Thus, they serve only as a mechanical support for the centre conductor of the coaxial line; of course this limits the usable bandwidth to some extent, as can be appreciated in Fig. 8*b*. This Figure shows the simulated response [10] for just the feed line structure for the Ka-band filter. This bandwidth is more than adequate for the narrowband filters studied. If wider bandwidths are required, a wideband coaxial transmission line using the same stubs can be found in [5].

The square coaxial structure is made out of five planar copper layers, which are machined, aligned and compressed together to form the three-dimensional coaxial structure. For this layered coaxial filter design, or for any general stub supported multilayer coaxial circuit, layer misalignment should be considered in both the design and fabrication technique. Layer misalignment for the filter presented in this paper is critical between layer 3 and layers 2 and 4, because it can modify three characteristics of the transmission line filter; the first one is the bandwidth, as misalignment can slightly modify the dimensions of the resonator in the middle of the structure changing the coupling between resonant modes. The second one is the frequency shift of the mechanical supports, since modification of the effective lengths of the quarter-wavelength stubs will modify the usable bandwidth. The third one is the characteristic impedance of the coaxial line, which can be changed by layer misalignments. The assembly of the coaxial filters is shown in Fig. 1*a*. For the Ka-band filter, all layers are 0.7 mm thick, and the overall enclosed dimensions of the filter are

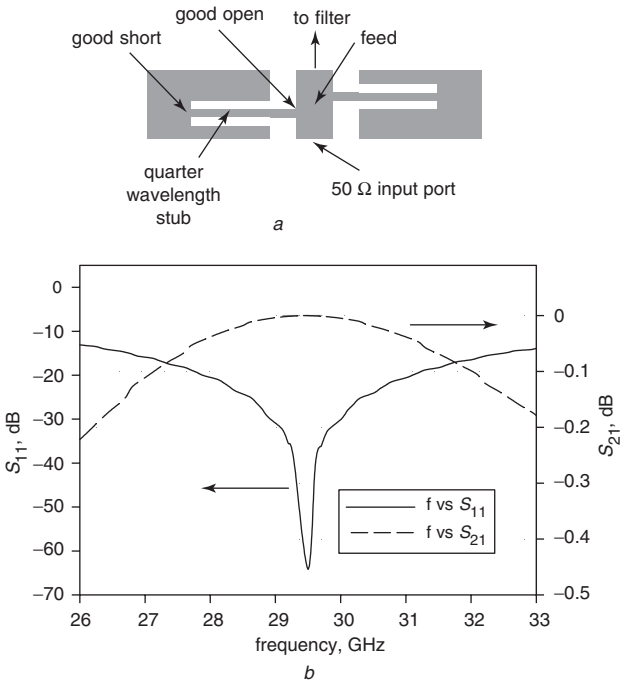

Fig. 8 *Feed of the dual-mode filter*
a Layout
b Response

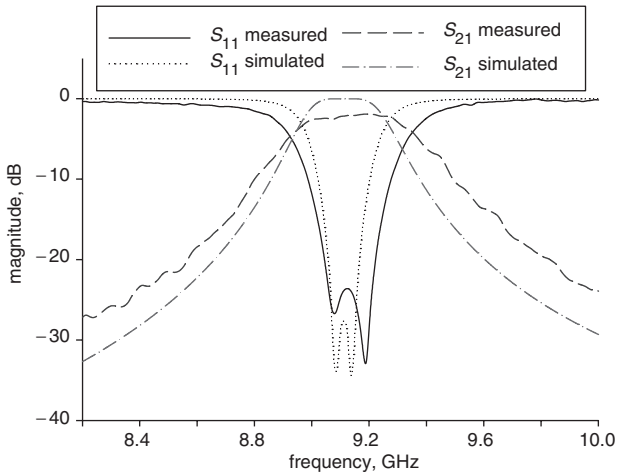

Fig. 9 *Response of the dual-mode X-band filter*

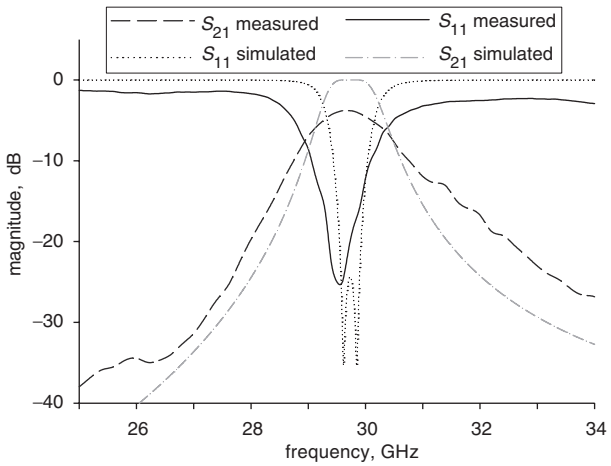

Fig. 10 *Response of the Ka-band filter*

14 mm × 7.5 mm × 2.1 mm. For the X-band filter, all layers are 2 mm thick, and the overall enclosed dimensions are 40 mm × 25 mm × 6 mm.

The X-band filter was produced by conventional machining, as the minimum dimension to mill was 1 mm. However the Ka-band filter requires high precision machining, making conventional machining impossible to use since dimensions need to be kept within a few microns tolerance. The minimum dimensions were 0.2 mm for the filter and 0.1 mm for the K connector interface. The 0.1 mm value was carefully determined in order to obtain the appropriate external Q-value. For this particular filter, laser machining was used which was able to provide the required small holes with an excellent accuracy. The filter plates were clamped together for both filters. Other methods of construction for integrated coaxial devices are metal-coated thick resists, such as SU8 [3], or metal-coated reactive-ion-etched silicon wafers [12, 13].

The band-pass response of the dual-mode X-band filter is shown in Fig. 9 where a good agreement between theory and experiment can be observed. The measured bandwidth increased due to layer misalignment, which slightly changed the coupling between the two modes.

The band-pass response of the dual-mode Ka-band filter is shown in Fig. 10 where a reasonable agreement between theory and experiment can be observed. An increase in the losses of this filter can be seen which is believed to be caused by the surface roughness of the copper plates, combined with a reduction in the quality of the copper, caused by the laser machining process. We are currently investigating alternative of microfabrication techniques [14] with the objective of finding a method of microfabrication which can produce high quality conductive layers out of which we can form the coaxial structure. The return loss was degraded due to layer misalignment, which also changed the coupling between the two modes, leading to an increase in the bandwidth of the filter. The transition from the connector to the circuit presented a small mismatch, which was mainly caused by fabrication tolerances at the time of mounting the connectors to the complete layered circuit. Nevertheless, this new type of filter has been effectively implemented.

4 Conclusions

Layered coaxial transmission line assembly presents a practical way of making low-loss microwave circuits, which are compact in size. From this structure two dual-mode narrowband filters were demonstrated. Microfabrication or micromachining methods were devised to satisfy the design tolerances and layer finishing requirements to produce quality air-filled coaxial devices for millimetre-wave operation. Furthermore, millimetre-wave passive components such as filters, antennas, coupling structures, delay lines and phase shifters can be easily matched and integrated using the multilayered low loss compact coaxial structure.

5 References

1 Blondy, P., Brown, A.R., Cros, D., and Rebeiz, G.M.: 'Low loss micromachined filters for millimetre wave communication systems', *IEEE Trans. Microw. Theory Tech.*, 1998, **46**, (12), pp. 2283–2288
2 Brown, A.R., and Rebeiz, G.M.: 'A high performance integrated K-band diplexer', *IEEE Trans. Microw. Theory Tech.*, 1999, **47**, (8), pp. 1477–1481
3 Harriss, J.E., Pearson, L.W., Wang, X., Barron, C.H., and Pham, A.V.: 'Membrane-supported Ka band resonator employing organic micromachined packaging', *IEEE MTT-S Int. Microw. Symp. Dig.*, 2000, pp. 1225–1228
4 Llamas-Garro, I.: 'Micromachined microwave filters'. PhD Thesis, University of Birmingham, UK, August 2003
5 Llamas-Garro, I., Lancaster, M.J., and Hall, P.S.: 'A low loss wideband suspended coaxial transmission line', *Microw. Opt. Technol. Lett.*, 2004, **43**, pp. 93–95
6 Gruner, L.: 'Higher order modes in square coaxial lines', *IEEE Trans. Microw. Theory Tech.*, 1983, **31**, (9), pp. 770–772
7 Lau, K.H.: 'Loss calculations for rectangular coaxial lines', *IEE Proc. H, Microw. Antennas Propag.*, 1998, **135**, (3), pp. 207–209
8 Rizzi, P.A.: 'Microwave engineering passive circuits' (Prentice Hall Inc, 1988)
9 Pozar, D.M.: 'Microwave engineering' (John Wiley and Sons Inc, 1998)
10 Ansoft HFSS, http://www.ansoft.com
11 Hong, J.-S., and Lancaster, M.J.: 'Microstrip filters for RF microwave applications' (John Wiley and Sons Inc, 2001)
12 Shimizu, S., Kuribayashi, K., Ohno, M., Taniguchi, T., and Ueda, T.: 'Low temperature reactive ion etching for bulk micromachining'. Proc. IEEE Symp. on Emerging Technologies and Factory Automation, 6-10 Nov 1994, pp. 48–52
13 Marxer, C., and de Rooij, N.F.: 'Micro-opto-mechanical 2 × 2 switch for single-mode fibers based on plasma-etched silicon mirror and electrostatic actuation', *J. Lightw. Technol.*, 1999, **17**, (1), pp. 2–6
14 Llamas-Garro, I., Jiang, K., Jin, P., and Lancaster, M.J.: 'SU-8 microfabrication for a Ka band filter'. Proc. 4th Workshop on MEMS for Millimeterwave Communications, LAAS-CNRS, Toulouse, France, 2–4 July 2003, pp. F55–F58